Applied Scientific Research **49**: 175–187, 1992

Flutter of slender bodies under axial stress

R. COENE

Department of Aerospace Engineering, Delft University of Technology, Delft, The Netherlands

Received 18 June 1990; accepted in revised form 27 May 1991

Abstract. The equations of motion of flexible slender bodies with constant body sections immersed in a uniform axial flow are discussed and used to derive some simple results for the divergence speed and the flutter speed. The results are compared with a classical waving flag result in two-dimensional flow. The slender body result for the flutter speed is compared with values obtained from wind tunnel experiments for some low budget paper strips.

1. Introduction

In Milne-Thomson's book 'Theoretical Hydrodynamics' [1] the problem of a two dimensional flapping flag is formulated in two examples, 18 and 19, in chapter XV as follows:

'18. Two portions of a large uniform stream of liquid of density ρ, flowing with velocity U, are separated by a plane boundary of perfectly flexible fabric, of mass m per unit area, and subject to a tension T, the boundary being parallel to the stream. Show that waves of length λ can be propagated along the fabric, in the direction of the stream, with a velocity V given by

$$mV^2 - T + \frac{\lambda\rho}{\pi}(U - V)^2 = 0, \tag{1.1}$$

provided that

$$T\left(1 + \frac{m\pi}{\lambda\rho}\right) > mU^2. \tag{1.2}$$

19. Explain, giving the necessary theory, why a flag flaps in a breeze'.

In this paper the slender body problem corresponding to the waving flag problem referred to above is treated. Solutions corresponding to (1.1) and (1.2) will be derived for flexible slender bodies with arbitrary cross-sections which are invariable in the streamwise direction. For cases with nearly neutral buoyancy (i.e. with the density of the body nearly equal to the density of the surrounding fluid) the results are relevant

to the readily observed wavy motions of weeds in a river. We also obtain some results for the divergence and flutter of a beam supported at both ends. Here divergence is the steady state aeroelastic instability and the term flutter is used for the oscillatory instability in a potential flow which involves no separation.

In the present context some general remarks on slender body theory are in order. Here a body is called slender if the local thickness in all directions perpendicular to the stream, is small with respect to the length in the direction of the undisturbed stream. A body whose local thickness is small in one direction only is called thin. Thus a line is the limit of a slender body as the thickness tends to zero, while the limit of a thin body is a surface. Whenever a slender body is laterally compressed the body may be both thin and slender, the result being a slender wing.

An essential feature of the slender body-approximation is that the velocity potential which describes the flow outside the boundary layer satisfies the two-dimensional Laplace equation in the near field. (In the far field the flow is dominated by a three-dimensional dipole). Satisfying certain conditions of smoothness in the streamwise direction solutions are readily obtained for many flow regimes of practical interest. The idea to use the concept of virtual momentum of a lateral section is due to Munk [2]. The same method is also applicable to unsteady flow problems. An interesting example of such an application is due to Lighthill [3] who explains the swimming of slender fish. The theory indicates that efficient propulsion can be generated by a wave of increasing amplitude which passes down the body at a phase velocity V slightly larger than the swimming speed U. At the sharp trailing edge a weak Joukowski condition, which allows for a finite pressure jump, is being satisfied while vorticity is being shed into the wake. Positive thrust can only be generated at a positive rate of working by the body. Conversely, a negative rate of working by the body is associated with drag. This case, of course, is related to 'flutter' and instability of motion.

In [4] and [5] the dynamics and the stability of towed flexible cylinders is discussed. Modes of oscillation are obtained for neutrally buoyant cylinders allowing for viscous effects and a variable tension in the bodies, keeping the nose of the body fixed in a steady stream. Surprisingly no reference is made in [4] and [5] to the fundamental results (1.1) and (1.2) or their slender body counterparts.

The stability problem and the voluntary swimming problem, where the body experiences a propulsive force by actively generating a wave passing down the body, are not the only ones which may lead to waves in a body.

As shown in [6] a wavy stream leads to a passive recoil mode with a phase velocity equal to the phase velocity of the oncoming waves when there is no tension in the body. Another example is a flag waving in the von Karman vortex street of the mast, where the wave velocity is dictated by the phase velocity at which the alternating vortices are convected downstream. In this paper, however, we consider the stability problem of slender bodies with constant tension and invariable body sections to derive the slender body counterpart of (1.1) and (1.2). Some experimental values for

the flutter speeds [7] of three strips of paper will be compared with the slender body results.

2. The equations of motion

We consider a flexible slender body in a uniform oncoming flow. A Cartesian coordinate system (x, y, z) which is an inertial system has its x-axis aligned with the oncoming flow velocity U. The body has length l and lateral dimensions which are small with respect to l (Fig. 2.1).

The cross-sections may perform displacements $h(x, t)$ in the vertical z-direction. Moreover, the z-x plane is a plane of symmetry of the body (Fig. 2.2). Therefore the flow is also symmetrical and there will be no torsional moments. The z-axis is a principal axis of the body sections and we assume a bending stiffness EI. We neglect deformations due to shear.

For the lateral (z-component) force exerted by the fluid on the body per unit length in the x-direction we use the classical slender body result [3]:

$$L(x, t) = -\rho\left(\frac{\partial}{\partial t} + U\frac{\partial}{\partial x}\right)(wA), \tag{2.1}$$

where ρ is the density of the fluid, and w is the resultant cross-flow with

$$w = \frac{\partial h}{\partial t} + U\frac{\partial h}{\partial x}. \tag{2.2}$$

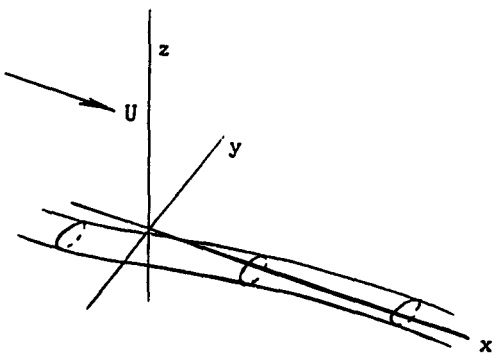

Fig. 2.1. The coordinate system.

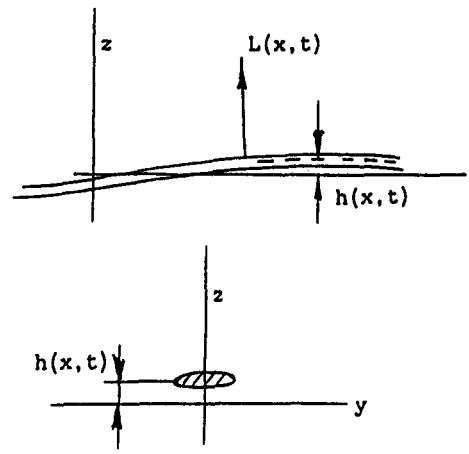

Fig. 2.2. The lateral displacements and the lateral force.

ρA is the virtual mass of the cross-sections for motions in the z-direction. The virtual mass (per unit length in the x-direction) is defined by

$$\rho A = \rho \oint_x \phi \, dy, \tag{2.3}$$

where ϕ is the velocity potential of the two-dimensional cross-flow when the cross-section moves at unit velocity in the z-direction. This quantity can be obtained from complex-variable theory of two-dimensional irrotational flow. For an elliptic section, of any excentricity, with axes a and b, moving in the direction of the a axis, one obtains

$$A = \frac{\pi}{4} b^2, \tag{2.4}$$

which is independent of a and therefore also valid for a flat plate with $a = 0$. For $a = b$, (2.4) is equal to the cross-sectional area of the circular cross-section. One may also observe that for $a < b$, A is given by the cross-sectional area of the smallest possible circular cylinder which circumscribes the section.

The differential operator $(\partial/\partial t + U(\partial/\partial x))$ appearing in (2.1) and (2.2) is the linearized approximation of the material derivative; i.e. a time derivative following a particle. Thus the right-hand side of (2.1) stands for the material time derivative of the z-component of momentum of a slice of fluid of unit thickness in the x-direction. One may write, neglecting the x-component of the velocity perturbations with respect to U:

$$\frac{D}{Dt} = \frac{\partial}{\partial t} + U \frac{\partial}{\partial x}, \tag{2.5}$$

for the time derivative in a coordinate system travelling at speed U in the positive x-direction with respect to the body. Obviously this coordinate system is fixed with respect to the fluid which is undisturbed far from the body. Equation (2.1) is valid for smooth variations in the x-direction and by virtue of the physical significance of (2.5) it is obvious that both w and A may depend on x and t. In this paper, however, only w is dependent on x and t while A is assumed to be constant. This restriction is not important for the validity of (2.1) but it is relevant to what follows. It implies that the expression on the right-hand side of (2.1) involves only second derivatives of $h(x, t)$ with respect to x and t and this, in turn, leads to the possibility of simple solutions which exhibit some interesting features.

By virtue of (2.1) the differential equation for $h(x, t)$, equating the rate of change of lateral momentum to the forces, becomes

$$(\rho_b S) \frac{\partial^2 h}{\partial t^2} = \frac{\partial}{\partial x}\left(T \frac{\partial h}{\partial x}\right) - \frac{\partial^2}{\partial x^2}\left(EI \frac{\partial^2 h}{\partial x^2}\right) - \left(\frac{\partial}{\partial t} + U \frac{\partial}{\partial x}\right)(\rho w A), \tag{2.6}$$

where the first three terms are the usual contributions for a vibrating beam, with

ρ_b the mass density of the body;
S the area of the cross-sections;
T the axial tension;
EI the flexural rigidity.

Assuming constant $\rho_b S = \sigma$, constant EI, constant T and constant $\rho A = \alpha$, equation (2.6) simplifies to

$$\sigma \frac{\partial^2 h}{\partial t^2} = T \frac{\partial^2 h}{\partial x^2} - EI \frac{\partial^4 h}{\partial x^4} - \alpha \left(\frac{\partial}{\partial t} + U \frac{\partial}{\partial x} \right)^2 h. \tag{2.7}$$

This is a fourth order linear equation for $h(x, t)$ involving only second and fourth order derivatives. This opens the way for wave solutions of exponential growth.

3. Exponentially growing wave solutions

Equation (2.7) has solutions of the form

$$h(x, t) = a\, e^{i(kx - \omega t)}, \tag{3.1}$$

where a is the amplitude in the steady oscillation case and the wavenumber k is related to the wavelength by $k = 2\pi/\lambda$; ω is the circular frequency.

Substitution of (3.1) into (2.7) yields a quadratic equation for ω (with $a \neq 0$):

$$-\sigma\omega^2 = -Tk^2 - EIk^4 - \alpha(-\omega^2 - U^2k^2 + 2\omega Uk), \tag{3.2}$$

which is solved by

$$\omega_{1,2} = \frac{k}{\alpha + \sigma}(\alpha U \pm \sqrt{(T + k^2 EI)(\alpha + \sigma) - \alpha\sigma U^2}). \tag{3.3}$$

Equating the discriminant in (3.3) to zero yields the critical situation:

$$T + k^2 EI - \frac{\alpha\sigma}{\alpha + \sigma} U^2 = 0. \tag{3.4}$$

If the left-hand side in (3.4) is positive one has the possibility of steady oscillations. If it is negative one has the possibility of exponential growth, i.e. flutter.

Starting from the critical situation (3.4) we distinguish three cases:

(a) In the absence of external flow, with $U = 0$, (3.4) cannot be satisfied with positive values of T. In what follows we shall come back to the case with negative values of T.

(b) Putting $T = 0$ in (3.4) yields a unique wavelength ($\lambda = 2\pi/k$):

$$\lambda = \frac{2\pi}{U}\sqrt{\frac{\alpha+\sigma}{\alpha\sigma}EI}, \tag{3.5}$$

and the corresponding frequency

$$\omega = \frac{\alpha U^2}{\alpha+\sigma}\sqrt{\frac{\alpha\sigma}{\alpha+\sigma}\frac{1}{EI}}, \tag{3.6}$$

and wavespeed

$$V = \frac{\omega}{k} = \frac{\alpha U}{\alpha+\sigma} < U. \tag{3.7}$$

(c) For a body with negligible rigidity, of perfectly flexible fabric, but also in the limit $k \to 0$, one obtains a unique flutter speed, U_{cr}, for given T with

$$U_{cr}^2 = \frac{\alpha+\sigma}{\alpha\sigma}T, \tag{3.8i}$$

or alternatively, a critical tension T_{cr} for given U,

$$T_{cr} = \frac{\alpha\sigma}{\alpha+\sigma}U^2. \tag{3.8ii}$$

We note that in this case the wave speed is also given by (3.7):

$$V = \frac{\omega}{k} = \frac{\alpha U}{\alpha+\sigma} < U, \tag{3.8iii}$$

but λ and ω are indeterminate.

For a waving weed with a circular cross-section and neutral buoyancy ($\alpha = \sigma$) in a river the wave speed which follows from (3.7) is one half the flow speed: $V = \frac{1}{2}U$. Obviously, the present analysis does not apply to the behaviour of the weeds after the onset of actual flutter, nor to large amplitude waves with variable stress and viscous effects but personal observations suggest that $V = \frac{1}{2}U$ might not be too far off.

The results (3.8) explain why the trailing part of a banner towed by an aircraft will generally be unstable. Adding a drag device behind the banner which increases the tension above the value (3.8ii) would stabilize the banner and increase its lifetime. The added drag due to the extra device is not a pure loss since a flapping banner with $V < U$ has a larger drag than a quiescent banner. The results (3.8) can be obtained in a slightly different way which sheds some light on the physical background. Putting $EI = 0$ in (2.7) and thereby retaining only the second order derivatives, equation (2.7) can be expressed as

$$\left(\frac{\partial}{\partial t} + c_1 \frac{\partial}{\partial x}\right)\left(\frac{\partial}{\partial t} + c_2 \frac{\partial}{\partial x}\right) h = 0, \tag{3.9}$$

with

$$c_1 c_2 = -\frac{T - \alpha U^2}{\alpha + \sigma}, \tag{3.10}$$

and

$$c_1 + c_2 = \frac{2\alpha U}{\alpha + \sigma}. \tag{3.11}$$

From (3.10) and (3.11) one readily obtains

$$c_{1,2} = \frac{\alpha U}{\alpha + \sigma} \pm \sqrt{\left(\frac{\alpha U}{\alpha + \sigma}\right)^2 + \frac{T - \alpha U^2}{\alpha + \sigma}}. \tag{3.12}$$

The discriminant in (3.12) vanishes with

$$T = \frac{\alpha \sigma}{\alpha + \sigma} U^2, \tag{3.13}$$

and the two phase velocities are then equal:

$$c_1 = c_2 = \frac{\alpha U}{\alpha + \sigma}. \tag{3.14}$$

The flutter speed which follows from (3.13) is the same as obtained before, in (3.8), and arises when two waves have the same phase velocity (3.14). From (3.10) we note that with

$$T = \alpha U^2, \tag{3.15}$$

which is larger than the critical value (3.8ii), one of the phase velocities, say c_1, vanishes and one finds:

$$c_1 = 0 \quad \text{and} \quad c_2 = \frac{2\alpha U}{\alpha + \sigma}. \tag{3.16}$$

At the special value (3.15) for the tension, a steady deformation $h(x)$, with $\partial h/\partial t = 0$, of arbitrary shape is possible. Thus, from (3.15) we obtain a divergence speed given by

$$U_{\text{div}}^2 = \frac{T}{\alpha}. \tag{3.17}$$

We note that this divergence speed is smaller than the flutter speed given by (3.8i) since

$$U_{\text{cr}}^2 = \frac{\alpha + \sigma}{\sigma} U_{\text{div}}^2 \quad \text{and} \quad \frac{\alpha + \sigma}{\sigma} > 1,$$

although for $\alpha \ll \sigma$ the two will be close together.

It is easily verified that equations (3.15) and (3.17) can be derived directly from equation (2.7) by putting the time derivatives equal to zero. Retaining the flexural rigidity then yields, with $T = -P$,

$$(P + \alpha U^2) \frac{\partial^2 h}{\partial x^2} + EI \frac{\partial^4 h}{\partial x^4} = 0. \tag{3.18}$$

Thus, e.g. Euler's buckling formula for a doubly pinned beam of length l ($l = \lambda/2$) can be supplemented with an apparent mass effect for exterior flow as

$$P_{\text{cr}} = \frac{\pi^2 EI}{l^2} - \alpha U^2. \tag{3.19i}$$

For a given value of the compression force one also obtains the divergence speed given by

$$\alpha U_{\text{div}}^2 = \frac{\pi^2 EI}{l^2} - P. \tag{3.19ii}$$

4. The two dimensional analogy

In the two dimensional case, referred to in the introduction, we start from a wave

potential in the form

$$\phi^+ = -ac\,e^{-kz}\cos[k\{x-(U+c)t\}]. \tag{4.1}$$

It is easily verified that (4.1) satisfies the two dimensional Laplace equation and vanishes for $z \to +\infty$ where we have uniform flow at speed U in the x-direction.

The $+$ indicating the upperside of the flag. At the lower side one has $\phi^- = -\phi^+$. $(U+c)$ is the phase speed of the wave and k is, again, the wavenumber, related to the wavelength λ by $k=2\pi/\lambda$.

At $z=0^+$, the boundary condition becomes

$$w = \frac{\partial h}{\partial t} + U\frac{\partial h}{\partial x} = \left(\frac{\partial \phi}{\partial z}\right)_{(z=0)} = -k\phi^+_{(z=0)}. \tag{4.2}$$

For the lateral force per unit surface we have from the linearized Bernoulli equation:

$$L(x,t) = -2p^+_{(z=0)} = 2\rho\left(\frac{\partial}{\partial t} + U\frac{\partial}{\partial x}\right)\phi^+_{(z=0)} = -2\rho ac^2 k\sin[k\{x-(U+c)t\}]. \tag{4.3}$$

From (4.2) and (4.3) we obtain

$$\left(\frac{\partial}{\partial t} + U\frac{\partial}{\partial x}\right)^2 h = -k\left(\frac{\partial}{\partial t} + U\frac{\partial}{\partial x}\right)\phi^+_{(z=0)} = -\frac{kL}{2\rho}. \tag{4.4}$$

With $k=2\pi/\lambda$, the lateral force may be expressed in terms of the wavelength:

$$L(x,t) = -\frac{\lambda\rho}{\pi}\left(\frac{\partial}{\partial t} + U\frac{\partial}{\partial x}\right)^2 h. \tag{4.5}$$

Equating the rate of change of vertical momentum to the vertical component of the force, this leads to an equation of motion analogous to (2.7) with $EI = 0$,

$$m\frac{\partial^2 h}{\partial t^2} = T\frac{\partial^2 h}{\partial x^2} - \frac{\lambda\rho}{\pi}\left(\frac{\partial}{\partial t} + U\frac{\partial}{\partial x}\right)^2 h, \tag{4.6}$$

where m is the mass per unit area of the fabric, as in (1.1).

With

$$\alpha = \frac{\lambda\rho}{\pi}, \tag{4.7}$$

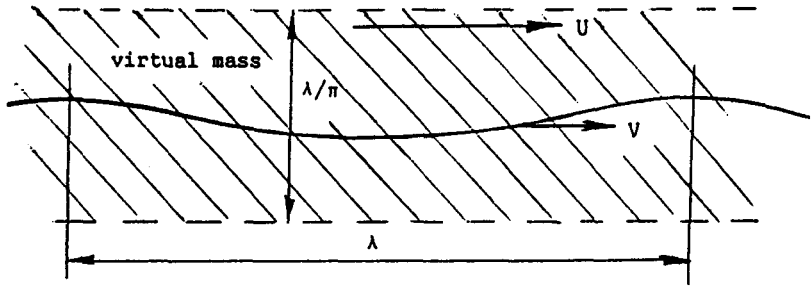

Fig. 4.1. The virtual mass in the two dimensional case.

the analogy with the slender body case is established. This leads to an interpretation of the coefficient $\lambda\rho/\pi$ in the two dimensional case which is somewhat unusual. Apparently the term $\lambda\rho/\pi$ plays the role of a virtual mass. A layer of fluid with thickness λ/π is effectively involved in the two dimensional flag case, see Fig. 4.1. In contrast with the slender body case this term is wavelength dependent.

Neglecting the flexural rigidity in equation (3.2) and putting $\omega/k = V$, we obtain

$$\sigma V^2 - T + \alpha(U - V)^2 = 0. \tag{4.8}$$

By virtue of (4.7) equation (4.8) is equivalent to (1.1) and (1.2) is implied. We note that the slender body results of Section 3 are more general than the two dimensional result in the sense that the cross-sections of the slender bodies need only be symmetrical with respect to the z-x plane, while there is no need for them to be laterally compressed, or 'thin'.

Moreover, we note that in the two dimensional case there are no unique speeds. The wave speed, the divergence speed and the flutter speed are wavelength-dependent, while the wavelength is indeterminate. In the slender body case these three speeds are uniquely determined but the wavelength and the corresponding frequency, being inversely proportional are also indeterminate in the free-free problems for a perfectly flexible body or foil.

5. Experimental results

The results (3.8) for the flutter speed and the critical tension will be compared with some experimental results for three strips of paper with different spans. These strips were mounted in the M-tunnel of the Aerospace Department in Delft, as indicated in Fig. 5.1. The test section of the M-tunnel is $0.40 \times 0.40\,\mathrm{m}^2$ and the speed range used was from 7 m/s to 16 m/s.

The end conditions for the strips were of the free-free type; the cable mountings restrained the strips only in the streamwise direction. The weights attached to the trailing edges were used to vary the tension in the strips. The tensions applied were

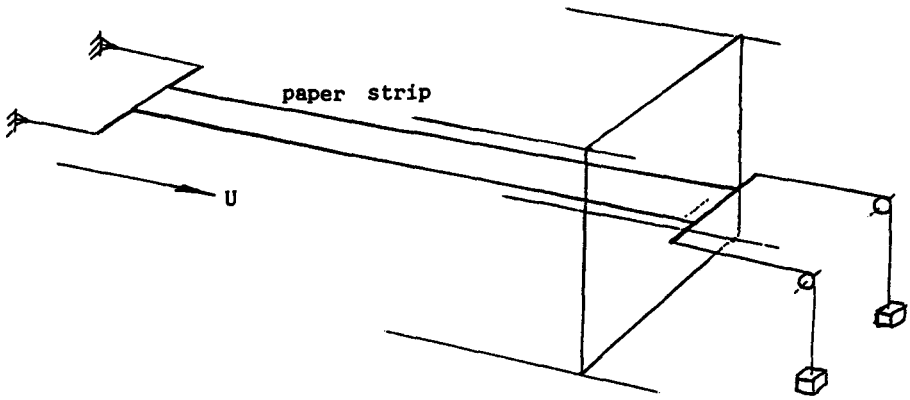

Fig. 5.1. The experimental set up.

sufficiently large with respect to the variations due to viscosity to justify the assumption of constancy of the tension. The length of the paper strips was 0.96 m. Three spans, 0.25 m, 0.165 m and 0.085 m were used. The mass density of the paper was 1.31×10^3 kg m^{-3}. The flexural rigidity was considered negligible, the thickness being 0.10×10^{-3} m. The tension applied went up to 2.6 N for the strip of largest span.

The following procedure was followed: weights were installed to adjust the tension. Then the wind tunnel speed was increased to the point where instability was observed. Then the tension and the corresponding dynamic pressures were plotted.

The results are given in Figs 5.2 and 5.3. In the latter the appropriate theoretical values are compared with the experimental values in terms of a referential tension defined by

$$T^* = U^2 \frac{\eta^2 \alpha_0 \sigma_0}{\eta \alpha_0 + \sigma_0}, \tag{5.1}$$

where η defines the span of a strip with respect to the span $b_0 = 0.085$ m of strip 3:

$$b = \eta b_0. \tag{5.2}$$

For α_0, the apparent mass per unit length of the reference strip, we have the mass of air enclosed by the circumscribed circular cylinder:

$$\alpha_0 = \rho \frac{\pi}{4} b_0^2 = 7.32 \times 10^{-3} \text{ kg/m},$$

and for σ_0 one has

$$\sigma_0 = 1.13 \times 10^{-2} \text{ kg/m}.$$

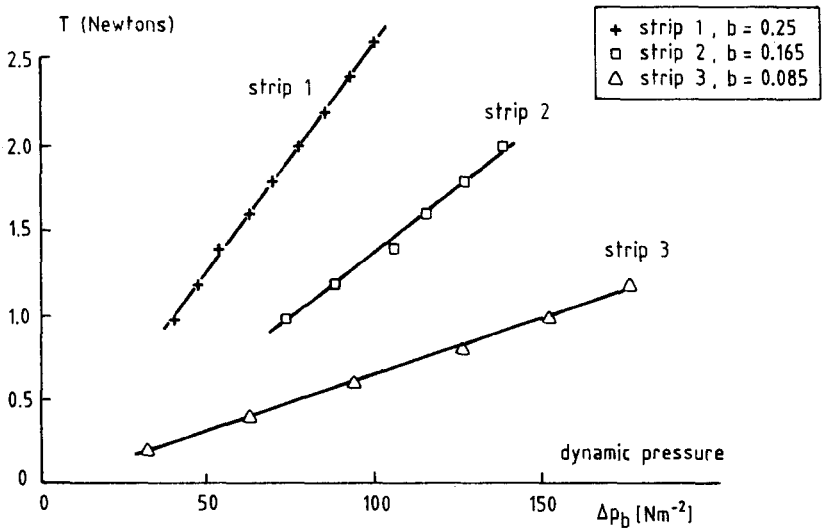

Fig. 5.2. The experimental results for the relation between the dynamic pressure $\Delta p_b = \frac{1}{2}\rho U^2$ and the tension in the strips at the trailing edge.

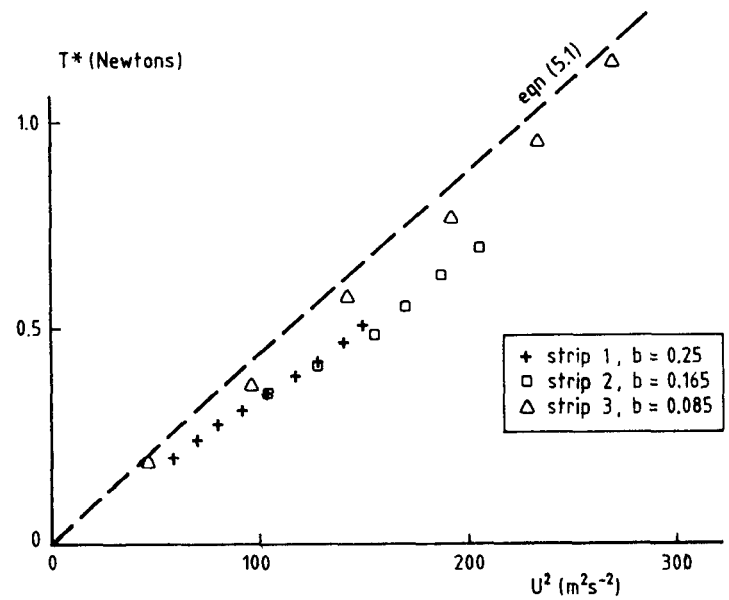

Fig. 5.3. Comparison of the theoretical T^* (equation 5.1) and the experiments with three strips. In fact, only strip 3 ($b/l = 0.09$) is 'slender'.

We note that the experimental results for strip 3 (span $b = 0.085$ m are closest to the theoretical prediction. Clearly strip 3 is 'more slender' than the other two.

6. Concluding remarks

From Fig. 5.2 it can be seen that the agreement of theory with experiment for strip 3, with aspect ratio $b/l = 0.09$, is satisfactory. The other strips, with $b/l = 0.17$ and 0.27, are not so slender and the agreement is less satisfactory. In all cases the critical speed is (safely) underpredicted. One reason is probably the neglect of viscous effects in the theory. In the experiments the tension due to the weights applied is only a minimum value at the trailing edge. The actual tension will slowly increase to some higher value (larger by the amount of the drag of the strip) at the leading edge. Thus one would expect the trailing part to be more unstable than the leading part. This however, could not be observed. Whenever flutter set in, the strip moved violently along the whole length.

Equation (3.8i) indicates that underpredicting U_{cr} may be due not only to underestimating T but also to overprediction of α. Strictly speaking, the value $\pi b^2/4$ (2.4) for the thin strip should be considered as an upper limit for l and λ tending to infinity. It may be noted that in the short wave limit, $\lambda/b \to 0$, the virtual mass α is given by (4.7) which vanishes with λ, rather than by (2.4). Obviously, only a more complete three dimensional lifting surface theory could match and incorporate both limits.

Acknowledgment

The experiments were carried out by two students, R.Y.C.M. Poland and A.J.J. Raayman, to whom the author expresses his gratitude.

References

1. Milne-Thomson, L.M., *Theoretical Hydrodynamics*, 5th edn. London: MacMillan (1968).
2. Munk, M.M., The aerodynamic forces on airship hulls. Report 184 (1923) NACA, pp. 451–468.
3. Lighthill, M.J., Note on the swimming of slender fish, *J. Fluid Mech.* 9 (1960) 305–317.
4. Paidoussis, M.P., Dynamics of flexible slender cylinders in axial flow, *J. Fluid Mech.* 26 (1966) 717–751.
5. Pao, H.P., Dynamical stability of a towed thin flexible cylinder, *J. Hydronautics* (1971) 144–150.
6. Coene, R., The swimming of flexible slender bodies in waves, *J. Fluid Mech.* 72 (1975) 289–303.
7. Raayman, A.J.J., Unpublished Report of the Department of Aerospace Engineering of the Delft University of Technology, TZ verslag TUD (1987).